Progress In Electromagnetics Research, PIER 67, 275–296, 2007

ON THE SPECTRAL EFFICIENCY OF A SPHERE

M. Gustafsson

Department of Electroscience
Lund University
Box 118, Lund, Sweden

S. Nordebo

School of Mathematics and System Engineering
Växjö University
Växjö, Sweden

Abstract—In many cases it is desired to have both high capacity and small antennas in wireless communication systems. Unfortunately, the antenna performance deteriorates when the antennas get electrically small. In this paper, fundamental limitations from antenna theory and broadband matching are used to analyze fundamental limitations on the spectral efficiency of an arbitrary antenna inserted inside a sphere.

1. INTRODUCTION

The spectral efficiency of a wireless communication system is determined by the properties of the channel that relates the transmitted and received signals. This communication channel is in general very complicated and depends on the feeding network, the antennas, and the wave propagation between the antennas. Recently, the multiple-input multiple-output (MIMO) systems have received much interest due to their ability to increase the spectral efficiency in wireless communication systems [6, 8, 23, 24, 31]. The MIMO systems are based on the use of multiple antennas at each end of the communication link in environments with rich multi-path propagation.

In many cases it is desired to design systems that have both a high capacity and a small physical size. Unfortunately, the antenna performance deteriorates when the antenna gets electrically small [14, 31]. Fundamental limitations on these kind of systems can be analyzed under various assumptions. The case with current

distributions and fields in free space are, e.g., discussed in [19, 21, 32]. In the planar case, a plane wave expansion shows that the fields are correlated at distances less than half the wavelength λ, giving a preferred antenna-array element spacing of approximately $\lambda/2$. Although, the volume formulation described in [21] can incorporate currents and fields, it is preferable to consider a model that includes the properties of the antennas. In this paper, fundamental limitations on the spectral efficiency of an arbitrary antenna inserted inside a sphere are analyzed.

To analyze the fundamental limitations of the spectral efficiency of a sphere, it is essential to relate three classical theories giving fundamental limitations in the disciplines of information theory, broadband matching, and antenna theory. In information theory, the Shannon theory set fundamental limits of how coding can be used to increase the data rate over a given communication channel, i.e., the capacity [28]. The capacity depends on the number and gain of the orthogonal sub channels and their signal to noise ratio [24]. For the spectral efficiency of a volume, the channel of interest relates the signals on transmission lines to the electromagnetic wave field outside the volume. Of course, this channel depends on the choice of antennas, matching, transmission lines, and the statistics of the radio channel outside the volume. Here, it is essential to consider the best possible antenna in the given volume as well as the best possible matching to a transmission line. The classical theory of broadband matching, shows how much power that can be transmitted between a transmission line and a given load [7], i.e., the antenna. The classical theory of radiation-Q uses spherical vector modes to analyze the properties of a hypothetical antenna inside a sphere [4, 14, 15, 34]. Multi-port antennas are considered in [9]. An antenna with a high Q-factor has electromagnetic fields with large amounts of stored energy around it, and hence, typically low bandwidth and high losses [14]. The mode expansion also gives a natural expression of the polarization, angle, and spatial diversity that is utilized in MIMO systems [6, 24, 29, 31].

The rest of the paper is organized as follows. In Section 2, a decomposition of the communication channel into a transmitting antenna channel, a wave propagation channel, and a receiving antenna channel is given. The antenna channels relate the electrical signals on transmission lines to the electromagnetic fields outside the antennas. The electromagnetic field is represented by spherical vector waves. In Section 3, it is shown that a set of unpolarized uniformly distributed plane waves impinging on the antennas can be represented by a Rayleigh channel in the spherical vector modes. In Section 4, the Fano theory is used to get fundamental limitations on the matching

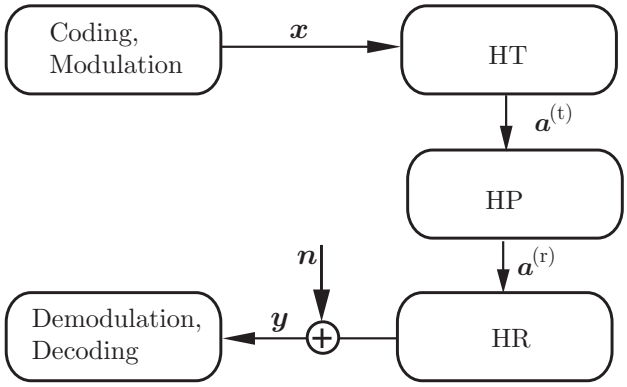

Figure 1. Block scheme of a wireless communication system. The received signal is $\boldsymbol{y} = \mathbf{H}\boldsymbol{x} + \boldsymbol{n}$, where the channel is decomposed into the parts $\mathbf{H} = \mathbf{H}_{\mathrm{R}}\mathbf{H}_{\mathrm{P}}\mathbf{H}_{\mathrm{T}}$ and $\boldsymbol{n}$ is the noise.

network for low order spherical vector modes and resonance circuits. The capacity of a Rayleigh fading antenna channel is analyzed in Section 5.

2. CHANNEL DECOMPOSITION AND SPHERICAL VECTOR MODE REPRESENTATION

A MIMO–model for a communication system with N_{x} transmitting antennas and N_{y} receiving antennas is considered, as depicted in Fig. 1. Here, $\boldsymbol{x}$ is the transmitted $N_{\mathrm{x}} \times 1$ signal, and $\boldsymbol{y}$ is the received $N_{\mathrm{y}} \times 1$ signal given by

$$\boldsymbol{y} = \mathbf{H}\boldsymbol{x} + \boldsymbol{n}, \tag{1}$$

where $\mathbf{H}$ is the complex $N_{\mathrm{y}} \times N_{\mathrm{x}}$ matrix, and $\boldsymbol{n}$ is uncorrelated complex Gaussian noise [22, 24, 31] with spectral density N_0. The total transmitted power is $P = \mathrm{trace}\{\mathbf{R}_{xx}\}$ where $\mathbf{R}_{xx}$ is the covariance matrix for the input signal $\boldsymbol{x}$.

To separate the antenna properties from the properties of the wave propagation, the communication channel is decomposed into a cascade of a transmitting antenna channel $\mathbf{H}_{\mathrm{T}}$, a wave propagation channel $\mathbf{H}_{\mathrm{P}}$, and a receiving antenna channel $\mathbf{H}_{\mathrm{R}}$, i.e., $\mathbf{H} = \mathbf{H}_{\mathrm{R}}\mathbf{H}_{\mathrm{P}}\mathbf{H}_{\mathrm{T}}$.

In particular, we can make the following assumptions: The communication distance is large enough so that there is no mutual coupling between the transmitting and receiving antenna arrays. The transmitted electric field $\boldsymbol{E}^{(\mathrm{t})}(\boldsymbol{r})$ can therefore be expanded in *outgoing*

spherical vector waves $\mathbf{u}^{(2)}_{\tau ml}(k\boldsymbol{r})$

$$\boldsymbol{E}^{(\mathrm{t})}(\boldsymbol{r}) = k\sqrt{2\eta}\sum_{l=1}^{\infty}\sum_{m=-l}^{l}\sum_{\tau=1}^{2} a^{(\mathrm{t})}_{\tau ml}\,\mathbf{u}^{(2)}_{\tau ml}\left(k(\boldsymbol{r}-\boldsymbol{r}_{\mathrm{t}})\right) \tag{2}$$

for $|\boldsymbol{r}-\boldsymbol{r}_{\mathrm{t}}| \geq R_{\mathrm{t}}$ where the propagation region is assumed to be source–free, $a^{(\mathrm{t})}_{\tau ml} = a^{(\mathrm{t})}_{\alpha}$ are the expansion coefficients, $\boldsymbol{r}_{\mathrm{t}}$ is the position of the transmitting antenna array, R_{t} the radius of a sphere containing the antenna, k the wave number, and η the free space impedance (see Appendix A). To simplify the notation, the multi–index $\alpha = (\tau, m, l)$ is used. Whenever necessary, the multi–index α is ordered and identified with the number $\alpha = 2(l^2 + l - 1 + m) + \tau$ [13]. The multi–poles are classified as either TE ($\tau = 1$) or TM ($\tau = 2$). The azimuthal and radial dependencies are given by the m and l index, respectively. The normalization with $k\sqrt{2\eta}$ is used to give a power normalization of the expansion coefficients, i.e., the totally radiated power is given by $\sum_{\alpha} |a^{(\mathrm{t})}_{\alpha}|^2$.

We assume that the transmitting antenna channel is given by a linear mapping from the input signal $\boldsymbol{x}$ to the expansion coefficients $a^{(\mathrm{t})}_{\alpha}$, and can therefore be represented as

$$\boldsymbol{a}^{(\mathrm{t})} = \mathbf{H}_{\mathrm{T}}\boldsymbol{x}, \tag{3}$$

where we employ a semi–infinite notation for the column vector $\boldsymbol{a}^{(\mathrm{t})} = [a^{(\mathrm{t})}_{\alpha}]$ and the matrix $\mathbf{H}_{\mathrm{T}}$ which has N_{x} columns.

We assume that the received electric field $\boldsymbol{E}^{(\mathrm{r})}(\boldsymbol{r})$ can be expanded in *incoming spherical vector waves* $\mathbf{u}^{(1)}_{\alpha}(k\boldsymbol{r})$

$$\boldsymbol{E}^{(\mathrm{r})}(\boldsymbol{r}) = \sqrt{2\eta}\,k\sum_{\alpha} a^{(\mathrm{r})}_{\alpha}\,\mathbf{u}^{(1)}_{\alpha}\left(k(\boldsymbol{r}-\boldsymbol{r}_{\mathrm{r}})\right) \tag{4}$$

for $|\boldsymbol{r}-\boldsymbol{r}_{\mathrm{r}}| \geq R_{\mathrm{r}}$, where $a^{(\mathrm{r})}_{\alpha}$ are the expansion coefficients, the multi–index $\alpha = (\tau, m, l)$ is employed, $\boldsymbol{r}_{\mathrm{r}}$ is the position of the receiving antenna array and R_{r} the radius of a sphere containing the antenna. The incoming spherical vector waves $\boldsymbol{v}_{\alpha}(k\boldsymbol{r})$ have the same basic features as the outgoing $\boldsymbol{u}^{(2)}_{\alpha}(k\boldsymbol{r})$ mentioned above.

The wave propagation channel $\mathbf{H}_{\mathrm{P}}$ contains the properties of the geometrical and electrical features between the transmitting antenna and the receiving antenna. In particular, the channel $\mathbf{H}_{\mathrm{P}}$ represents the mapping from the transmitted electric field $\boldsymbol{E}^{(\mathrm{t})}(\boldsymbol{r})$ to the received electric field $\mathbf{E}^{(\mathrm{r})}(\boldsymbol{r})$, or equivalently, the mapping from the expansion

coefficients $a_\alpha^{(\mathrm{t})}$ to $a_\alpha^{(\mathrm{r})}$. We assume that this mapping is linear, and can therefore be represented as

$$\boldsymbol{a}^{(\mathrm{r})} = \mathbf{H}_{\mathrm{P}} \boldsymbol{a}^{(\mathrm{t})}, \tag{5}$$

where the matrix $\mathbf{H}_{\mathrm{P}}$ is (countably) infinite–dimensional in both rows and columns. In practice however, and as we will see later, this matrix can be considered finite and represents as many modes that are practically relevant. The bandwidth of higher order modes will ultimately tend to zero as the corresponding Q-factors tend to infinity, and these modes will therefore not contribute to the capacity of the communication channel.

We assume that the receiving antenna channel is given by a linear mapping from the expansion coefficients $a_\alpha^{(\mathrm{r})}$ to the received signal $\boldsymbol{y}$, and can hence be represented as

$$\boldsymbol{y} = \mathbf{H}_{\mathrm{R}} \boldsymbol{a}^{(\mathrm{r})}, \tag{6}$$

where the semi–infinite matrix $\mathbf{H}_{\mathrm{R}}$ has N_{y} rows. Finally, the received signal $\boldsymbol{y}$ is corrupted by white Gaussian noise (1).

3. THE RAYLEIGH FADING ANTENNA CHANNEL

The Rayleigh channel is defined as a channel with uncorrelated and zero mean entries having complex Gaussian distribution and the amplitudes thus being Rayleigh distributed [22, 24, 25, 31], i.e., $\mathbf{H} = \mathbf{H}_{\mathrm{w}}$, where $\mathcal{E}\{\mathbf{H}_{\mathrm{w}}\} = 0$ and $\mathcal{E}\{\mathbf{H}_{\mathrm{w}}|_{ij} \mathbf{H}_{\mathrm{w}}^*|_{mn}\} = \delta_{im}\delta_{jn}$. However, it is also customary to derive this property from the assumption that a large number of independent and uniformly distributed scattered waves are incident on the receiver, see e.g., [17]. In this Section, we show that a set of unpolarized uniformly distributed plane waves impinging on the antennas can be represented as a Rayleigh channel in the spherical modes.

Consider the channel from the transmitted signals to the received spherical vector modes, i.e., $\mathbf{H}_{\mathrm{P}}\mathbf{H}_{\mathrm{T}}$. Suppose that the received electric field (4) is given by

$$\boldsymbol{E}^{(\mathrm{r})}(\boldsymbol{r}) = \sum_{n=1}^{N_{\mathrm{s}}} s_n \boldsymbol{E}_n \mathrm{e}^{-\mathrm{i}k\hat{\boldsymbol{k}}_n \cdot (\boldsymbol{r} - \boldsymbol{r}_{\mathrm{r}})} \tag{7}$$

for $|\boldsymbol{r} - \boldsymbol{r}_{\mathrm{r}}| \geq R_{\mathrm{r}}$, consisting of a number of uniformly distributed and independent scattered plane wave components. Here s_n represents the complex signal amplitudes, $\boldsymbol{E}_n$ random field strengths, and the time convention $\mathrm{e}^{\mathrm{i}\omega t}$ is used.

It is assumed that for each fixed direction $\hat{\boldsymbol{k}}_n$, the field $\boldsymbol{E}_n$ has zero-mean complex Gaussian components with the variance E_0^2, i.e., $\boldsymbol{E}_n = E_0(\phi_1\hat{\boldsymbol{u}}_1 + \phi_2\hat{\boldsymbol{u}}_2)$, where $\hat{\boldsymbol{u}}_1$ and $\hat{\boldsymbol{u}}_2$ are two orthogonal unit vectors that are perpendicular to $\hat{\boldsymbol{k}}_n$ and the Gaussian variables ϕ_i, $i = 1, 2$ have unit variance. This means that the polarization of $\boldsymbol{E}_n$ is uniformly distributed over the Poincare sphere, i.e., *unpolarized*, with the *Stokes parameter* $E_0^2 = \mathcal{E}\left\{|\boldsymbol{E}_n|^2\right\}$. The average power flux is given by $E_0^2/(2\eta)$. It is furthermore assumed that the incident directions $\hat{\boldsymbol{k}}_n$ are uniformly distributed over the unit sphere.

The wave propagation channel $\mathbf{H}_{\mathrm{P}}$ can be decomposed into two parts $\mathbf{H}_{\mathrm{P}} = \mathbf{H}_{\mathrm{A}}\mathbf{H}_{\mathrm{B}}$ where $\mathbf{H}_{\mathrm{B}}$ represents the mapping from $a_\alpha^{(\mathrm{t})}$ to s_n coefficients, and $\mathbf{H}_{\mathrm{A}}$ represents the mapping from s_n coefficients to $a_\alpha^{(\mathrm{r})}$. Thus,

$$\boldsymbol{a}^{(\mathrm{r})} = \mathbf{H}_{\mathrm{A}}\boldsymbol{s} \tag{8}$$

where the mapping (8) is defined by the expansion of plane waves in incoming spherical vector waves

$$a_\alpha^{(\mathrm{r})} = \frac{1}{\sqrt{2\eta}\,k}\sum_{n=1}^{N_{\mathrm{A}}} 2\pi \mathrm{i}^{1-\tau-l}\,\mathbf{A}_\alpha^*(\hat{\boldsymbol{k}}_n)\cdot\boldsymbol{E}_n s_n, \tag{9}$$

where $\mathbf{A}_\alpha$ denote the spherical vector harmonics (see Appendix). Hence, we can conclude that

$$\mathbf{H}_{\mathrm{A}}|_{\alpha n} = \frac{2\pi}{\sqrt{2\eta}\,k}\mathrm{i}^{1-\tau-l}\,\mathbf{A}_\alpha^*(\hat{\boldsymbol{k}}_n)\cdot\boldsymbol{E}_n. \tag{10}$$

The channel $\mathbf{H}_{\mathrm{A}}$ is a random channel. With the assumption above of uniformly distributed unpolarized waves, the expectation of each channel element is zero, i.e., $\mathcal{E}\left\{\mathbf{H}_{\mathrm{A}}|_{\alpha n}\right\} = 0$. The expectation of the channel product elements $\mathbf{H}_{\mathrm{A}}|_{\alpha n}\mathbf{H}_{\mathrm{A}}^*|_{\alpha' n'}$ can be written

$$\begin{aligned}
&\mathcal{E}\left\{\mathbf{H}_{\mathrm{A}}|_{\alpha n}\mathbf{H}_{\mathrm{A}}^*|_{\alpha' n'}\right\}\\
&= \frac{2\pi^2}{\eta k^2}\mathrm{i}^{l'-l+\tau'-\tau}\mathcal{E}\left\{\mathbf{A}_\alpha^*(\hat{\boldsymbol{k}}_n)\cdot\boldsymbol{E}_n\,\mathbf{A}_{\alpha'}(\hat{\boldsymbol{k}}_{n'})\cdot\boldsymbol{E}_{n'}^*\right\}\\
&= \frac{2\pi^2}{\eta k^2}\mathrm{i}^{l'-l+\tau'-\tau}\mathcal{E}_{\hat{\boldsymbol{k}}}\left\{\mathbf{A}_\alpha^*(\hat{\boldsymbol{k}}_n)\cdot\mathcal{E}_{\boldsymbol{E}}\left\{\boldsymbol{E}_n\boldsymbol{E}_{n'}^*\right\}\cdot\mathbf{A}_{\alpha'}(\hat{\boldsymbol{k}}_{n'})\right\}.
\end{aligned} \tag{11}$$

The expectation over the polarization is

$$\mathcal{E}_{\boldsymbol{E}}\left\{\boldsymbol{E}_n\boldsymbol{E}_{n'}^*\right\} = \mathcal{E}\left\{|\boldsymbol{E}_n|^2\right\}\mathbf{I}_{2\times 2}\delta_{nn'} = E_0^2\mathbf{I}_{2\times 2}\delta_{nn'}, \tag{12}$$

where $\mathbf{I}_{2\times 2}$ denotes the 2-by-2 identity dyad. The expectation over the incident angles is hence

$$\begin{aligned}
&\mathcal{E}\left\{\mathbf{H}_{\mathrm{A}}|_{\alpha n}\mathbf{H}_{\mathrm{A}}^{*}|_{\alpha' n'}\right\} \\
&= \frac{2\pi^2 E_0^2}{\eta k^2}\mathrm{i}^{l'-l+\tau'-\tau}\mathcal{E}_{\hat{\boldsymbol{k}}}\left\{\mathbf{A}_{\alpha}^{*}(\hat{\boldsymbol{k}}_n)\cdot\mathbf{A}_{\alpha'}(\hat{\boldsymbol{k}}_n)\right\}\delta_{nn'} \\
&= \frac{\pi E_0^2}{2\eta k^2}\mathrm{i}^{l'-l+\tau'-\tau}\delta_{nn'}\int_{\Omega}\mathbf{A}_{\alpha}^{*}(\hat{\boldsymbol{r}})\cdot\mathbf{A}_{\alpha'}(\hat{\boldsymbol{r}})\,\mathrm{d}\Omega = \frac{\pi E_0^2}{2\eta k^2}\delta_{\alpha\alpha'}\delta_{nn'}. \qquad (13)
\end{aligned}$$

Here, it is essential to normalize the SNR to the total power of the electromagnetic wave that impinges on the sphere. It is also necessary to consider the distribution of the average amplitude as a function of frequency. We assume that the amplitude decay is proportional to the propagation distance in wavelengths, i.e., E_0/k is constant. The plane wave is normalized with respect to the power flux through the cross section of the sphere with radius $\lambda/(2\pi) = k^{-1}$. To simplify the notation, the average power per plane wave is defined as

$$\frac{P}{N_{\mathrm{s}}} = \frac{E_0^2\pi}{2\eta k^2}, \qquad (14)$$

where P is measure of the power on the receiver side. In conclusion, the fundamental Rayleigh channel $\mathbf{H}_{\mathrm{A}}$ defined in (7) though (9) has complex Gaussian entries, i.e., $\mathbf{H}_{\mathrm{A}} = \sqrt{P/N_{\mathrm{s}}}\mathbf{H}_{\mathrm{w}}$. The trace of the covariance matrix for the signal $\boldsymbol{s}$ is normalized as $\mathrm{trace}\{\mathbf{R}_{ss}\} = N_{\mathrm{s}}$.

The received signal is hence given by

$$\begin{aligned}
\boldsymbol{y} = \sqrt{\frac{P}{N_{\mathrm{s}}}}\mathbf{H}_{\mathrm{R}}\mathbf{H}_{\mathrm{w}}\boldsymbol{s} + \boldsymbol{n} &= \sqrt{\frac{P}{N_{\mathrm{s}}}}\mathbf{H}_{\mathrm{R}}\mathbf{H}_{\mathrm{w}}\mathbf{H}_{\mathrm{B}}\mathbf{H}_{\mathrm{T}}\boldsymbol{x} + \boldsymbol{n} \\
&= \sqrt{\frac{P}{N_{\mathrm{s}}}}\mathbf{H}_{\mathrm{R}}\mathbf{H}_{\mathrm{w}}\mathbf{R}_{\mathrm{T}}^{1/2}\boldsymbol{x} + \boldsymbol{n}, \qquad (15)
\end{aligned}$$

where $\mathbf{R}_{\mathrm{T}}^{1/2} = \mathbf{H}_{\mathrm{B}}\mathbf{H}_{\mathrm{T}}$ is the correlation matrix [24] on the transmitter side. It is also observed that $\mathbf{H}_{\mathrm{R}}$ can be interpreted as the square root of the correlation matrix on the receiver side, i.e., $\mathbf{H}_{\mathrm{R}} = \mathbf{R}_{\mathrm{R}}^{1/2}$.

In the analysis of the receiving channel $\mathbf{H}_{\mathrm{R}}$ the channel model from random plane waves $\boldsymbol{s}$ to $\boldsymbol{y}$ in (15) is used. This is equivalent to the assumption of an uncorrelated channel on the transmitter side $\mathbf{R}_{\mathrm{T}} = \mathbf{I}$. This gives the channel

$$\boldsymbol{y} = \sqrt{\frac{P}{N_{\mathrm{s}}}}\mathbf{H}_{\mathrm{R}}\mathbf{H}_{\mathrm{w}}\boldsymbol{s} + \boldsymbol{n}. \qquad (16)$$

A SVD of the receiving channel, $\mathbf{H}_{\mathrm{R}} = \mathbf{U}\boldsymbol{\Sigma}'\mathbf{V}^{\mathrm{H}}$, gives

$$\tilde{\boldsymbol{y}} = \mathbf{U}^{\mathrm{H}}\boldsymbol{y} = \sqrt{\frac{P}{N_{\mathrm{s}}}}\boldsymbol{\Sigma}'\mathbf{V}^{\mathrm{H}}\mathbf{H}_{\mathrm{w}}\boldsymbol{s} + \mathbf{U}^{\mathrm{H}}\boldsymbol{n}. \tag{17}$$

To simplify this channel model, we first observe that $\mathbf{V}^{\mathrm{H}}\mathbf{H}_{\mathrm{w}}$ is a semi-infinite Rayleigh matrix with N_{s} columns. Secondly, we let $\boldsymbol{\Sigma}$ denote the $N_{\mathrm{y}} \times N_{\mathrm{y}}$ diagonal matrix containing the singular values of the semi-infinite matrix $\boldsymbol{\Sigma}'$. Finally, the infinite matrix product in $\boldsymbol{\Sigma}'\mathbf{V}^{\mathrm{H}}\mathbf{H}_{\mathrm{w}}$ is replaced by a finite matrix product between $\boldsymbol{\Sigma}$ and a finite Rayleigh matrix. This gives the equivalent channel

$$\tilde{\boldsymbol{y}} = \sqrt{\frac{P}{N_{\mathrm{s}}}}\boldsymbol{\Sigma}\mathbf{H}_{\mathrm{w}}\boldsymbol{s} + \tilde{\boldsymbol{n}}, \tag{18}$$

where $\boldsymbol{\Sigma}$ and $\mathbf{H}_{\mathrm{w}}$ are an $N_{\mathrm{y}} \times N_{\mathrm{y}}$ diagonal matrix containing the singular values of $\mathbf{H}_{\mathrm{R}}$ and an $N_{\mathrm{y}} \times N_{\mathrm{s}}$ Rayleigh matrix, respectively.

Since the channel is random the corresponding information rate is a random variable. The capacity of these fading channels are commonly analyzed with the ergodic capacity and the outage capacity [24]. In this section, we do not consider the bandwidth of the system and hence use the capacity (efficiency) with the unit b/s/Hz as commonly used in MIMO literature. To avoid confusion with the capacity in b/s, we either give the units or use the word capacity efficiency whenever necessary.

The ergodic capacity (in b/s/Hz) of the channel (18) is given by

$$\overline{C} = \mathcal{E}\left\{\max_{\mathbf{R}_{ss}} \log_2 \det\left(\mathbf{I} + \frac{P}{N_0 N_{\mathrm{s}}}\boldsymbol{\Sigma}\mathbf{H}_{\mathrm{w}}\mathbf{R}_{ss}\mathbf{H}_{\mathrm{w}}^{\mathrm{H}}\boldsymbol{\Sigma}\right)\right\} \tag{19}$$

where $\boldsymbol{\Sigma}$ and $\mathbf{H}_{\mathrm{w}}$ are the diagonal matrix containing the singular values of $\mathbf{H}_{\mathrm{R}}$ and an $N_{\mathrm{y}} \times N_{\mathrm{s}}$ Rayleigh channel, respectively. The water-filling solution [24] can be used to determine the covariance matrix $\mathbf{R}_{ss}$ in (19), and hence the ergodic capacity.

The case of an idealized antenna connecting each spherical vector mode to one port gives N_{y} uncorrelated sub-channels $\boldsymbol{\Sigma} = \mathbf{I}_{N_{\mathrm{y}} \times N_{\mathrm{y}}}$. The ergodic capacity, in b/s/Hz, is given by the ergodic capacity of the $\mathbf{H}_{\mathrm{w}}$ channel, i.e.,

$$\overline{C} = \mathcal{E}\left\{\max_{\mathbf{R}_{ss}} \log_2 \det\left(\mathbf{I} + \frac{P}{N_0 N_{\mathrm{s}}}\mathbf{H}_{\mathrm{w}}\mathbf{R}_{ss}\mathbf{H}_{\mathrm{w}}^{\mathrm{H}}\right)\right\}. \tag{20}$$

The properties of this $\mathbf{H}_{\mathrm{w}}$ MIMO channel is analyzed in many papers,

see e.g., [24, 31]. A lower bound on the ergodic capacity is given by

$$\overline{C} \geq R \log_2 \left(1 + \frac{P}{N_0 N_\mathrm{s}} \exp \left(\frac{1}{R} \sum_{j=1}^{R} \sum_{p=1}^{R'} \frac{1}{p} - \gamma \right) \right) \tag{21}$$

where $R = \min(N_\mathrm{y}, N_\mathrm{s})$, $R' = \max(N_\mathrm{y}, N_\mathrm{s})$, and $\gamma = 0.577$ is Euler's constant [24]. It is seen that the capacity efficiency of an antenna that connects each spherical vector mode to one port increases rapidly with the number of ports as long as the SNR is sufficiently high. It is also observed that the capacity efficiency is independent of the radius of the antenna. Since the number of spherical modes is infinite, the number of spatial channels is also infinite irrespectively of the size of the volume. Obviously, this is unrealistic. To circumvent this problem the capacity over a certain bandwidth has to be considered.

The interpretation of the capacity (19) can be simplified by assuming a sufficiently high SNR, so that the identity matrix in (19) can be neglected. This gives

$$\overline{C} \approx \mathcal{E} \left\{ \log_2 \det \left(\frac{P}{N_0 N_\mathrm{s}} \mathbf{H}_\mathrm{w} \mathbf{R}_{ss} \mathbf{H}_\mathrm{w}^\mathrm{H} \right) \right\} + \log_2 \det \left(\mathbf{\Sigma}^2 \right). \tag{22}$$

The second term can be interpreted as the loss in ergodic capacity due to the antenna channel at a high SNR. The correlation loss is given by

$$\Delta\overline{C} = \log_2 \det \left(\Sigma^2 \right) = \log_2 \prod_{m=1}^{N_\mathrm{y}} \sigma_m^2 = \sum_{m=1}^{N_\mathrm{y}} \log_2 \sigma_m^2, \tag{23}$$

where σ_n denotes the singular values of Σ. Since the receiving antenna channel has a total power gain $\|\mathbf{\Sigma}\|_\mathrm{F}^2 \leq N_\mathrm{y}$ giving $\det \mathbf{\Sigma} \leq 1$ and hence $\Delta\overline{C} \leq 0$. $\Delta\overline{C}$ can be interpreted as a loss due to correlation on the receiver side [24].

4. LIMITATIONS ON THE ANTENNA CHANNEL

The antenna channels connect the electrical signals on the transmission line with the radiated electromagnetic waves outside the antenna. This channel is generally very complex. Here, the case where each transmission line is connected to a spherical wave with a lossless matching network is considered (see Fig. 2). From the input signal, the antenna can be modeled with a lumped circuit model. The spherical vector modes have an equivalent circuit representing the impedance of the modes [4, 15]. The equivalent circuits of the lowest order

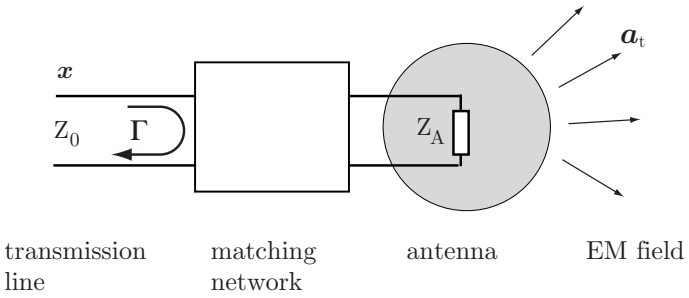

Figure 2. The transmitting (and receiving) antenna channel $\mathbf{H}_{\mathrm{T}}$ is the map from the electrical signals $\boldsymbol{x}$ on the transmission line to the radiated electromagnetic field outside the antenna, here represented by the spherical vector modes $\boldsymbol{a}_{\mathrm{t}}$.

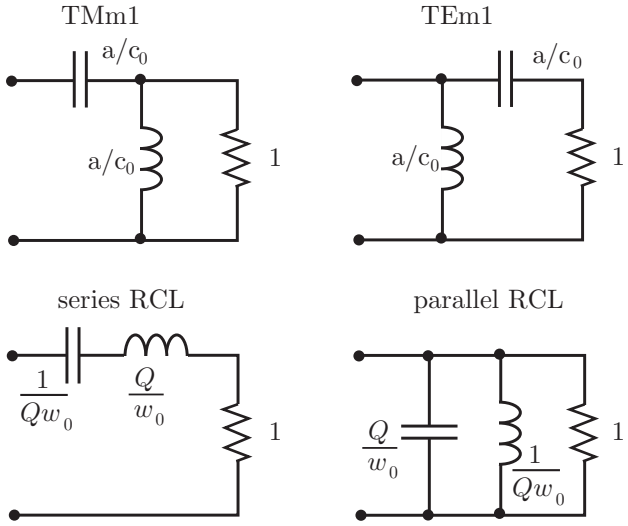

Figure 3. Circuit models of simple antennas. The resistor models the radiation part. The capacitor and inductor model the parts that store the electric field and magnetic field, respectively. The inductance and capacitance of the lowest order modes are given by a/c_0, where a and c_0 are the sphere radius and speed of light, respectively.

modes, i.e., the TM_{m1} and TE_{m1} for $m = -1, 0, 1$, are shown in Fig. 3. The resistance R, capacitance C, and inductance L are the circuit equivalents of the radiated field, the stored electric field, and the stored magnetic field, respectively. The higher order modes are

given by a ladder network [4, 15]. Here, the Fano theory is used to get fundamental limitations between the bandwidth and threshold level on the reflection coefficient for any realizable matching network [7, 11, 26, 30].

4.1. Impedance of TM and TE Modes

The Fano theory uses Taylor expansions of the reflection coefficient around the zeros of the transmission coefficient to get a set of integral relations for the reflection coefficient. Here, we assume that the transmission line has unit impedance. The transmission coefficient of the TM_{m1} and TE_{m1} modes has a double zero at $s = 0$. The corresponding reflection coefficient has no zeros but two poles, $\lambda_{\mathrm{p}1,2} = (-1 \pm \mathrm{i})/(2a/c_0)$. The coefficients of the Taylor series around $s = 0$ give the two integral relations

$$\frac{2}{\pi}\int_0^\infty \omega^{-2} \ln \frac{1}{|\Gamma(\mathrm{i}\omega)|}\,\mathrm{d}\omega = \left(\frac{2a}{c_0} - 2\sum_i \lambda_{\mathrm{r}i}^{-1}\right) \tag{24}$$

and

$$\frac{2}{\pi}\int_0^\infty \omega^{-4} \ln \frac{1}{|\Gamma(\mathrm{i}\omega)|}\,\mathrm{d}\omega = \left(\frac{4a^3}{3c_0^3} + \frac{2}{3}\sum_i \lambda_{\mathrm{r}i}^{-3}\right), \tag{25}$$

where the coefficients $\lambda_{\mathrm{r}i}$ have a positive real-valued part. It is noted that it is enough to consider one coefficient λ_{r} or a complex conjugated pair [7]. Assuming a constant reflection factor $2\ln\dfrac{1}{|\Gamma|} = \pi K$, over the bandwidth $|\omega - \omega_0| \le \omega_0 B/2$ gives

$$K\frac{B}{1 - B^2/4} = 2\xi - 2\frac{\omega_0}{\lambda_{\mathrm{r}}} \tag{26}$$

and

$$K\frac{B + B^3/12}{(1 - B^2/4)^3} = \frac{4\xi^3}{3} + \frac{2}{3}\frac{\omega_0^3}{\lambda_{\mathrm{r}}^3} \tag{27}$$

where $\xi = k_0 a = \omega_0 a/c_0$. These equations are solved numerically with respect to B and λ_{r}. The fractional bandwidth B is depicted for the reflection coefficient $|\Gamma| = 1/3$ in Fig. 4.

For the narrow bandwidth case $B \ll 1$, the equalities can be combined as

$$KB \le \frac{4\xi^3}{3} + \frac{2}{3}\left(\xi - \frac{KB}{2}\right)^3 \le 2(k_0 a)^3 - \xi^2 KB. \tag{28}$$

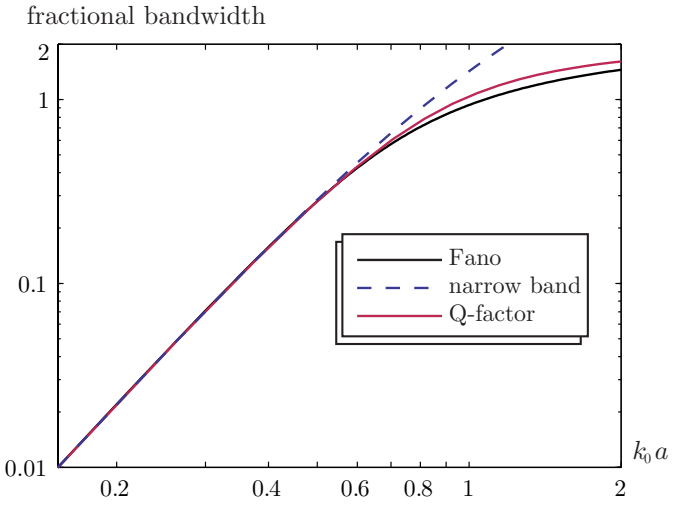

Figure 4. Fano fractional bandwidth of the TM_{m1} and TE_{m1} modes as function of the sphere radius $k_0 a$ for a reflection coefficient $|\Gamma| = 0.3$ (or SWR=2). Comparison between the Fano bandwidth given by (26) and (27), the narrowband approximation (29), and the Q-factor approximation (32).

This gives the asymptotic bandwidth

$$B \leq \frac{\pi}{\ln |\Gamma|^{-1}} \frac{\xi^3}{1+\xi^2} \quad \text{for } B \ll 1, \tag{29}$$

where we recognize the well known proportionality to $\xi^3/(1+\xi)$, i.e., the Q-factor of the TM_{m1} and TE_{m1} modes (also see Fig. 4).

4.2. Q-factor Approximation

In theory, the equivalent circuits can be used to derive a Fano bandwidth for any TM_{ml} or TE_{ml} mode. However, this is rather tedious due to the complex structure of these higher order modes together with the non-linearity of the Fano theory. Moreover, it is known that it is advantageous to mix the TE and TM modes in high bandwidth systems [15]. Instead of using the analytic expression of the impedance it is common to use the Q-factor (quality factor, antenna Q or radiation Q) to get an estimate of the bandwidth. Since there is an extensive literature on the Q-factor for antennas, see e.g., [4, 5, 8–11, 14, 15, 34, 40], only some of the results are given here. The Q

of the antenna is defined as the quotient between the power stored in the reactive field and the radiated power [4, 15]. The Q-factor is proportional to the bandwidth of the corresponding resonance circuit as $B \sim Q^{-1}$ for $Q \gg 1$. The Q-factor can either be determined by the equivalent circuits [4, 15] or by an analytic expression functions [5]. The Q of the TM_{ml} or TE_{ml} mode is given by

$$Q = \xi + \frac{\xi}{2R}\left(\frac{l(l+1)}{\xi^2} - \frac{X}{\xi} - X^2 - R^2\right), \tag{30}$$

where $R + \mathrm{i}X = \mathrm{i}(\xi\,\mathrm{h}_l^{(2)}(\xi))'/(\xi\,\mathrm{h}_l^{(2)}(\xi))$ and $\mathrm{h}_l^{(2)}$ denotes the spherical Hankel function [5, 11]. The Q-factor depends only on the l-index and there are $2(2l+1)$ modes for each l index, see Fig. 5a. The six lowest order modes have $Q = \xi^{-3} + \xi^{-1}$. By combination of one TE_{m1} mode and one TM_{m1} mode the Q-factor is reduced to $Q = \xi^{-3}/2 + \xi^{-1}$, see also [9] for a discussion of multi-port antennas.

The impedance of the spherical vector modes can be approximated with the impedance of a resonance circuit around the resonance frequency, $\omega_0 = 2\pi f_0$, see Fig. 3 and [11]. For frequencies around the resonance frequency, the radiated power is given by $P_{\mathrm{rad}} = |T|^2 P_{\mathrm{in}} = (1 - |\Gamma|^2)P_{\mathrm{in}}$. The transmission coefficient of the RCL circuits in Fig. 3 has a single zero at the origin and a single zero at infinity. The minimal reflection coefficient for a given fractional bandwidth and vise versa are easily determined with the Fano theory [7, 11, 26]. The reflection coefficient and the transmission coefficient are bounded as

$$|\Gamma| \geq \mathrm{e}^{-\frac{\pi}{QB}(1-B^2/4)} \quad \text{and } |T|^2 \leq 1 - \mathrm{e}^{-\frac{2\pi}{QB}(1-B^2/4)}, \tag{31}$$

respectively (see also Fig. 5b). The corresponding bound on the fractional bandwidth is

$$B \leq \sqrt{Q^2K^2 + 4} - QK \approx \frac{\pi}{Q \ln |\Gamma|^{-1}}, \tag{32}$$

where we recognize the well known proportionality $B \sim 1/Q$. However, the bound (32) gives the proportionality constant in terms of the reflection coefficient $|\Gamma|$. Also, observe that the Q-factor approximation agrees with the narrowband result in (29), see Fig. 4. This justifies the use of the Q-factor approximation to estimate the bandwidth of the first spherical vector modes. In [11], it is shown that the Q-factor approximation is accurate for the higher order spherical vector modes if Q is large.

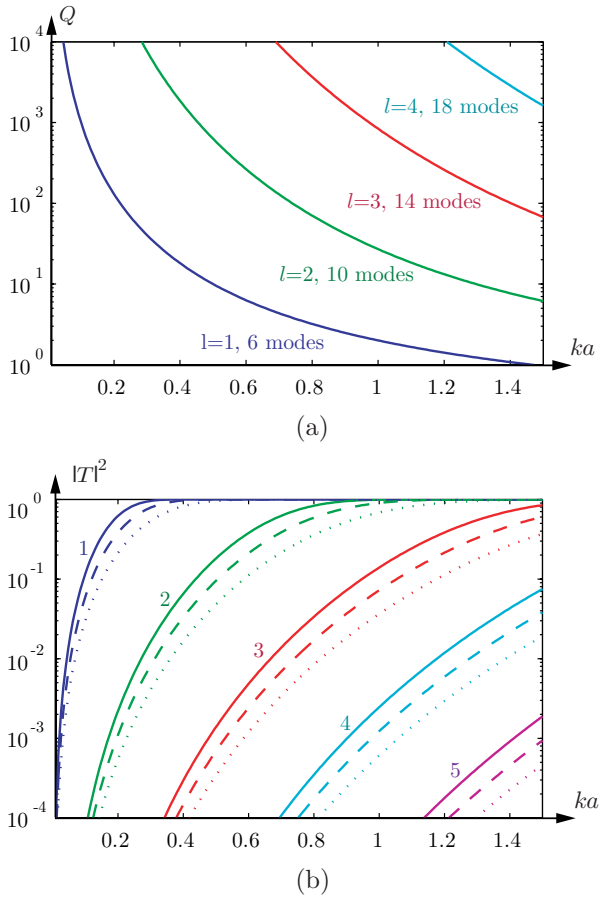

Figure 5. (a) Q-factor as a function of the sphere radius ka, (b) transmission coefficient $|T|^2$ in (31) as a function of ka for bandwidths of 5%, 10%, and 20%.

5. CAPACITY OF A SPHERE IN A RAYLEIGH CHANNEL

In this Section, we analyze how the fundamental limitations derived in Section 4 affect the capacity of a sphere. We use the signal model of (18) over a fixed bandwidth Δf. The ergodic capacity, in b/s, is given by

$$\overline{C}_{\Delta f} = \mathcal{E}\Big\{ \int_{f_1}^{f_2} \max_{\mathbf{R}_{ss}} \log_2 \det \left(\mathbf{I} + \frac{P_{\rm tot} \mathbf{\Sigma} \mathbf{H}_{\rm w} \mathbf{R}_{ss} \mathbf{H}_{\rm w}^{\rm H} \mathbf{\Sigma}^{\rm H}}{N_0 N_{\rm s} \Delta f} \right) {\rm d}f \Big\}, \quad (33)$$

where $P_{\text{tot}}/(N_{\text{s}}\Delta f)$ is the average power per plane wave and Hz. The matrix $\mathbf{R}_{ss}$ is given by the space–frequency water-filling solution [24, 31]. The communication scheme can, e.g., be the OFDM [2, 3, 27]. To simplify the analysis, we consider the capacity efficiency over a bandwidth B, i.e.,

$$\overline{C}_{\text{B}} = \mathcal{E}\left\{\max_{\mathbf{R}_{ss}} \log_2 \det\left(\mathbf{I} + \frac{P\boldsymbol{\Sigma}\mathbf{H}_{\text{w}}\mathbf{R}_{ss}\mathbf{H}_{\text{w}}^{\text{H}}\boldsymbol{\Sigma}^{\text{H}}}{N_0 N_{\text{s}}}\right)\right\}, \tag{34}$$

where $P = P_{\text{tot}}/\Delta f$ is the power density. The matrix $\mathbf{R}_{ss}$ is given by the water-filling solution [24, 31] and, hence, $\overline{C}_{\Delta f} \geq \overline{C}_B \Delta f = \overline{C}_B B f_0$.

In contrary to the fixed frequency case (21) where the singular values could be chosen to unity in the uncorrelated case, the singular values in (33) are limited by the required bandwidth. The Fano limit (31) on the reflection factor shows that the singular values are bounded by

$$\sigma_n^2 = 1 - |\Gamma_n|^2 = 1 - \mathrm{e}^{-\frac{2\pi}{Q_n B}(1-B^2/4)}, \tag{35}$$

where Q_n is the Q-factor of port number n. Here, one observes that the singular values σ_n^2 are small if the product between the Q-factor and the fractional bandwidth is large. The classical bandwidth definition of SWR = 2 corresponds to a singular value $\sigma_n^2 = 8/9$.

We consider the case with no channel knowledge, $\mathbf{R}_{ss} = \mathbf{I}$, where the Jensen inequality can be used to estimate the capacity [33], i.e.,

$$\begin{aligned}\overline{C}_{\text{B}} \leq C_{\text{BJ}} &= \log_2 \det\left(\mathbf{I} + \frac{P\boldsymbol{\Sigma}\mathcal{E}\left\{\mathbf{H}_{\text{w}}\mathbf{H}_{\text{w}}^{\text{H}}\right\}\boldsymbol{\Sigma}^{\text{H}}}{N_0 N_{\text{s}}}\right) \\ &= \sum_{n=1}^{N_{\text{y}}} \log_2\left(1 + \frac{P}{N_0}\sigma_n^2\right).\end{aligned} \tag{36}$$

The upper bound C_{BJ}, in b/s/Hz, is deterministic, independent of N_{s}, and depends only on the properties of the receiving antenna channel and the SNR. For the case of a large number of uncorrelated incident waves, i.e., N_{s} large, the inequality (36) becomes an equality since $\mathbf{H}_{\text{w}}\mathbf{R}_{ss}\mathbf{H}_{\text{w}}^{\text{H}} = \mathbf{H}_{\text{w}}\mathbf{H}_{\text{w}}^{\text{H}} \to N_{\text{s}}\mathbf{I}_{N_{\text{y}}\times N_{\text{y}}}$ as $N_{\text{s}} \to \infty$. Observe that the estimate of (36) is not good for $N_{\text{y}} > N_{\text{s}}$, as it overestimates the capacity by giving same results as for $N_{\text{y}} \ll N_{\text{s}}$. With the Fano estimate, (35), of the singular values, we get

$$C_{\text{BJ}} = \sum_{n=1}^{N_{\text{y}}} \log_2\left(1 + \frac{P}{N_0}\left(1 - \mathrm{e}^{-\frac{2\pi}{Q_n B}\left(1-\frac{B^2}{4}\right)}\right)\right) \tag{37}$$

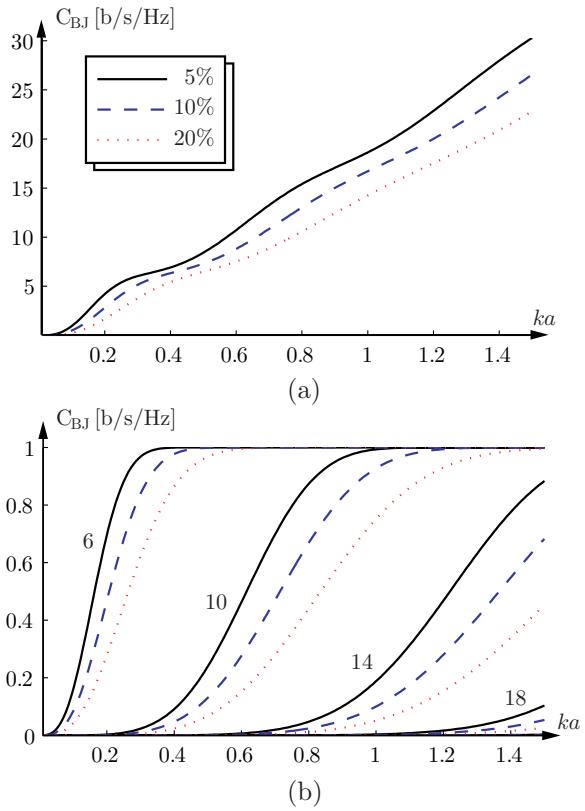

Figure 6. Capacity efficiency C_{BJ} of an idealized mode coupled antenna as a function of the radius ka for the bandwidths 5%, 10%, and 20% estimated with (37). (a) the capacity efficiency, (b) the capacity efficiency of each mode.

as an expression of the capacity efficiency over a bandwidth B for N_{s} large. Here, we observe that the capacity is limited by the product $Q_n B$.

For the idealized antenna connecting one spherical vector mode to one port, the explicit representation of the Q-factors can be used to calculate (37). The capacity C_{BJ} as a function of the sphere radius is depicted in Fig. 6a for the bandwidths 5%, 10%, and 20%, an SNR of $P/N_0 = 1$, and an infinite number of antenna ports $N_{\mathrm{y}} = \infty$. As seen in the figure, the capacity efficiency decreases with increased bandwidth. The capacity, in b/s, increases due to the multiplication with the bandwidth. It is also seen that the capacity increases rapidly with the size of the sphere. This is due the increased spatial diversity of

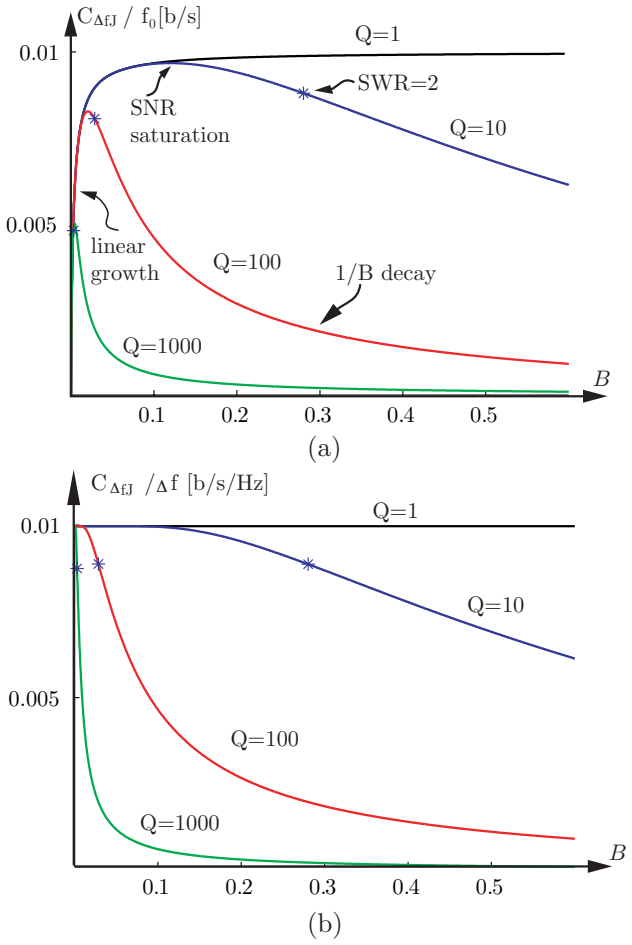

Figure 7. The capacity $C_{\Delta \mathrm{fJ}}$ as a function of the bandwidth for different Q-factors. The bandwidths related to $|\Gamma| = 1/3$ are indicated by the stars. (a) the capacity in b/s with fixed total power $P_{\mathrm{tot}}/(N_0 f_0) = 0.01$. (b) the capacity efficiency (in b/s/Hz) with fixed power density $P/N_0 = 0.01$.

the idealized antenna as seen in Fig. 6b, where the capacity efficiency of each subchannel is shown. Only the first 6 modes, corresponding to $l = 1$, are used for a small sphere. For a larger sphere, the higher order modes can also be used.

It is also interesting to consider how the capacity, in b/s, for a fixed volume depends on the bandwidth. In this case it is natural to

consider the total power $P_{\text{tot}} = P\Delta f$ as fixed, this gives

$$\frac{C_{\Delta \text{fJ}}}{f_0} = B \sum_{n=1}^{N_{\text{y}}} \log_2 \left(1 + \frac{P_{\text{tot}} \left(1 - \mathrm{e}^{-\frac{2\pi}{Q_n B} \left(1 - \frac{B^2}{4} \right)} \right)}{N_0 f_0 B} \right). \tag{38}$$

The capacity (b/s) divided by the center frequency in (38) is plotted in Fig. 7 for the scaled signal to noise ratio $P_{\text{tot}}/(N_0 f_0) = 0.01$. Three regions can by identified in the figure. For sufficiently small fractional bandwidths BN_{y}, the capacity increases approximately linearly with BN_{y}. This is the region where MIMO systems have a large advantage, i.e., the capacity increases almost linearly with the number of spatial channels N_{y}. For larger bandwidths the power in each channel gets small and the capacity is limited by the SNR. Finally, the capacity deceases due to the large mismatch of the antenna.

6. CONCLUSIONS

The analysis of the spectral efficiency in this paper reveals that it is important to consider a model that incorporates the properties of the antennas and the matching network. As shown in (21), the ergodic capacity at a fixed frequency, i.e., capacity in b/s/Hz, is independent of the size of the sphere. This means that, at least in theory, it would be possible to design small antenna with high spatial diversity. The drawback of small antennas such as being narrowband and lossy are well known [14, 31]. These drawbacks are naturally included in the analysis by consideration of the capacity over a bandwidth, i.e., capacity in b/s. We can also conclude that it is very efficient to utilize the polarization diversity for small antennas.

The analysis is based on several assumptions. The Rayleigh type channel is widely used in the literature and it is also used here due to its simple closed form solutions. It is straightforward to include a line of sight giving a Ricean channel [24]. However, even this is probably too simple for a realistic MIMO channel model. It would be interesting to consider more realistic MIMO channel and to determine how angular, spatial, and polarization diversity relates to mode diversity. The use of spherical vector modes to model an arbitrary antenna is standard in antenna theory. Here, we assume that each mode or a simple linear combination of modes is connected to one port by a lossless matching network. This lets us use the Fano theory to relate the bandwidth to the reflection coefficient of the system. For future work, it would be interesting to include an arbitrary multi-port matching network. It should also be observed that in practice it is very difficult to reach

the considered limit as it is very difficult to reach any of them, i.e., Shannon capacity in coding, Fano limit in broadband matching, and Q limitations in antenna design.

ACKNOWLEDGMENT

The financial support by the Swedish research council is gratefully acknowledged. The authors express their gratitude to Prof. George Papanicolaou for the opportunity to visit his group at the Mathematics Department, Stanford University, during March 2003, and the many fruitful discussions on wave propagation and statistical signal processing from which the present paper has emanated.

APPENDIX A. SPHERICAL VECTOR WAVES

An arbitrary electromagnetic field can be expanded in outgoing and incoming spherical vector waves [1, 12, 13, 16]

$$\boldsymbol{E}(\boldsymbol{r}) = k\sqrt{2\eta}\sum_{l=1}^{\infty}\sum_{m=-l}^{l}\sum_{\tau=1}^{2} a_{\tau ml}\,\mathbf{u}_{\tau ml}^{(2)}(k\boldsymbol{r}) + b_{\tau ml}\,\mathbf{u}_{\tau ml}^{(1)}(k\boldsymbol{r}) \qquad \text{(A1)}$$

where the time convention $\mathrm{e}^{\mathrm{i}\omega t}$ is used. The terms labeled by $\tau = 1$, l, and m identify magnetic 2^l-poles and the terms labeled by $\tau = 2$, l, and m identify electric 2^l-poles. The incoming, $\mathbf{u}^{(1)}$, and outgoing, $\mathbf{u}^{(1)}$, spherical vector waves are given by

$$\mathbf{u}_{1ml}^{(n)}(k\boldsymbol{r}) = \mathrm{h}_l^{(n)}(kr)\,\mathbf{A}_{1ml}(\hat{\boldsymbol{r}}) \qquad \text{(A2)}$$

$$\mathbf{u}_{2ml}^{(n)}(k\boldsymbol{r}) = \frac{1}{k}\nabla \times \left(\mathrm{h}_l^{(n)}(kr)\,\mathbf{A}_{1ml}(\hat{\boldsymbol{r}})\right) \qquad \text{(A3)}$$

where $\mathrm{h}_l^{(n)}, n = 1, 2$ denote the spherical Hankel functions and $\mathbf{A}$ denote the spherical vector harmonics. There are several common definitions of the spherical vector harmonics [1, 16]. For $\tau = 1, 2$, we use

$$\mathbf{A}_{1ml}(\hat{\boldsymbol{r}}) = \frac{1}{\sqrt{l(l+1)}}\nabla \times (\boldsymbol{r}\,\mathrm{Y}_l^m(\hat{\boldsymbol{r}})) \qquad \text{(A4)}$$

$$\mathbf{A}_{2ml}(\hat{\boldsymbol{r}}) = \hat{\boldsymbol{r}} \times \mathbf{A}_{1ml}(\hat{\boldsymbol{r}}), \qquad \text{(A5)}$$

where Y_l^m denotes the spherical harmonics [1, 16].

REFERENCES

1. Arfken, G., *Mathematical Methods for Physicists*, third edition, Academic Press, Orlando, 1985.
2. Bingham, J. A. C., "Multicarrier modulation for data transmission: An idea whose time has come," *IEEE Communications Magazine*, Vol. 28, 5–14, May 1990.
3. Blum, R. S., G. Y. Li, J. H. Winters, and Q. Yan, "Improved space-time coding for MIMO-OFDM wireless communications," *IEEE Transactions on Communications*, Vol. 49 No. 11, 1873–1878, Nov. 2001.
4. Chu, L. J., "Physical limitations of omni-directional antennas," *Appl. Phys.*, Vol. 19, 1163–1175, 1948.
5. Collin, R. E. and S. Rothschild, "Evaluation of antenna Q," *IEEE Trans. Antennas Propagat.*, Vol. 12, 23–27, Jan. 1964.
6. Driessen, P. F. and G. J. Foschini, "On the capacity formula for multiple input-multiple output wireless channels: A geometric interpretation," *IEEE Trans. on Communication*, Vol. 47, No. 2, 173–176, Feb. 1999.
7. Fano, R. M., "Theoretical limitations on the broadband matching of arbitrary impedances," *Journal of the Franklin Institute*, Vol. 249, Nos. 1, 2, 57–83 and 139–154, 1950.
8. Fante, R. L., "Quality factor of general antennas," *IEEE Trans. Antennas Propagat.*, Vol. 17, No. 2, 151–155, Mar. 1969.
9. Foltz, H. D. and J. S. McLean, "Bandwidth limitations on antenna systems with multiple isolated input ports," *Microwave Opt. Techn. Lett.*, Vol. 19, No. 4, 301–304, Nov. 1998.
10. Geyi, W., P. Jarmuszewski, and Y. Qi, "The foster reactance theorem for antennas and radiation Q," *IEEE Trans. Antennas Propagat.*, Vol. 48, No. 3, 401–408, Mar. 2000.
11. Gustafsson, M. and S. Nordebo, "Bandwidth, Q factor, and resonance models of antennas," *Progress In Electromagnetics Research*, PEIR 62, 1–20, 2006.
12. Gustafsson, M. and S. Nordebo, "Characterization of MIMO antennas using spherical vector waves," *IEEE Trans. Antennas Propagat.*, Vol. 54, No. 9, 2679–2682, 2006.
13. Hansen, J. E. (ed.), "Spherical near-field antenna measurements," *IEE Electromagnetic Waves Series*, No. 26, Peter Peregrinus Ltd., Stevenage, UK, 1988. ISBN: 0-86341-110-X.
14. Hansen, R. C., "Fundamental limitations in antennas," *Proc. IEEE*, Vol. 69, No. 2, 170–182, 1981.

15. Harrington, R. F., *Time Harmonic Electromagnetic Fields*, McGraw-Hill, New York, 1961.
16. Jackson, J. D., *Classical Electrodynamics*, second edition, John Wiley & Sons, New York, 1975.
17. Jakes, W. C. and D. Cox, *Microwave Mobile Communications*, IEEE Press, 1994.
18. Jensen, M. A. and J. W. Wallace, "A review of antennas and propagation for MIMO wireless communications," *IEEE Trans. Antennas Propagat.*, Vol. 52, No. 11, 2810–2824, Nov. 2004.
19. Loyka, S., "Information theory and electromagnetism: Are they related?" *COST 273/284 Workshop on Antennas and Related System Aspects in Wireless Communications*, Gothenburg, Sweden, June 2004.
20. McLean, J. S., "A re-examination of the fundamental limits on the radiation Q of electrically small antennas," *IEEE Trans. Antennas Propagat.*, Vol. 44, No. 5, 672–676, May 1996.
21. Miller, D. A. B., "Communicating with waves between volumes: Evaluating orthogonal spatial channels and limits on coupling strengths," *Appl. Opt.*, Vol. 39, No. 11, 1681–1699, Apr. 2000.
22. Miller, K. S., *Complex Stochastic Processes*, Addison-Wesley Publishing Company, Inc., 1974.
23. Molisch, A., *Wireless Communications*, John Wiley & Sons, 2005.
24. Paulraj, A., R. Nabar, and D. Gore, *Introduction to Space-Time Wireless Communications*, Cambridge University Press, Cambridge, U.K., 2003.
25. Proakis, J. G., *Digital Communications*, third edition, McGraw-Hill, 1995.
26. Pues, H. F. and A. R. V. D. Capelle, "An impedance-matching technique for increasing the bandwidth of microstrip antennas," *IEEE Trans. Antennas Propagat.*, Vol. 37, No. 11, 1345–1354, Nov. 1989.
27. Raleigh, G. G. and J. M. Cioffi, "Spatio-temporal coding for wireless communication," *IEEE Transactions on Communications*, Vol. 46, No. 3, 357–366, Mar. 1998.
28. Shannon, C. E., "A mathematical theory of communication," *Bell System Technical Journal*, Vol. 27, 379–423 and 623–656, July and October 1948.
29. Svantesson, T., "Correlations and channel capacity of MIMO systems employing multimode antennas," *IEEE Trans. Vehicular Technol.*, Vol. 51, No. 6, 1304–1312, 2002.
30. Vassiliadis, A. and R. L. Tanner, "Evaluating the impedance

broadbanding potential of antennas," *IRE Trans. on Antennas and Propagation*, Vol. 6, No. 3, 226–231, July 1958.

31. Vaughan, R. and J. Bach Andersen, *Channels, Propagation and Antennas for Mobile Communications*, Institution of Electrical Engineers, 2003.
32. Wallace, J. W. and M. A. Jensen, "Intrinsic capacity of the MIMO wireless channel," *Vehicular Technology Conference, 56th*, IEEE, Vol. 2, 701–705, 2002.
33. Wennström, M., "On MIMO systems and adaptive arrays for wireless communication," Ph.D. Thesis, Uppsala University, Sweden, 2002.
34. Yaghjian, A. D. and S. R. Best, "Impedance, bandwidth, and Q of antennas," *IEEE Transactions on Antennas and Propagation*, Vol. 53, No. 4, 1298–1324, 2005.